PROPERTIES OF SURFACE-MODIFIED COLLOIDAL PARTICLES

Joan M. Breiner[1],*, Michael A. Anderson[1], Harry W. K. Tom[2] and Robert C. Graham[1]

[1]Department of Environmental Sciences, University of California, Riverside, California 92521, USA
[2] Department of Physics, University of California, Riverside, California 92521, USA

Abstract—The reactivity of colloidal particles is regulated by their surface properties. These properties affect the wettability, flocculation-dispersion characteristics, ion exchange, sorption capacities and transport of inorganic colloids. Most studies have focused on hydrophilic, charged-particle surfaces, often ignoring the alterations in surface properties produced by the adsorption of natural organic matter, surfactants and other compounds. Adsorption of these substances can potentially render a surface substantially more hydrophobic. Nevertheless, comparatively little is known about changes in surface properties and reactivity of minerals upon sorption of hydrophobic organic compounds. In this study, the properties of four minerals (kaolinite, pyrophyllite, montmorillonite and Min-U-Sil®) and two inorganic materials (X-ray amorphous Al hydroxide and X-ray amorphous Si oxide) were compared before and after treatment with the common silylating agent, trimethylchlorosilane (TMCS). The samples were characterized by measurements of total carbon, cation exchange capacity (CEC), particle size, specific surface area (SSA), electrophoretic mobility, contact angle, particle aggregation, and by X-ray diffraction and diffuse reflectance infrared spectroscopy. For the layer silicates, surface coverage was limited to ~2% trimethyl silane (TMSi). TMSi covered 7.5% of the Min-U-Sil® surface and 33% of the X-ray amorphous Si oxide. Treatment did not affect the structure of the minerals but reduced the CEC, SSA and electrophoretic mobilities. Water contact angles increased to between 18 and 114° with treatment. While the apolar characteristic of the surfaces decreased minimally with treatment, the Lewis acid/base properties were substantially reduced and interfacial free energy shifted from positive to negative values indicating a more hydrophobic surface character. For all the samples except kaolinite, these changes affected the stability of the colloids in suspension depending upon solution pH. Although the grafting of TMSi altered colloidal mineral surface properties and increased their hydrophobicity, these changes were not sufficient to predict colloid aggregation behavior.

Key Words—Contact Angle, Hydrophobic Surface, Kaolinite, Montmorillonite, Pyrophyllite, Quartz, Trimethylchlorosilane.

INTRODUCTION

Colloidal particles are environmentally ubiquitous and influence a wide variety of environmental and industrial processes (Shaw, 1992; Stumm, 1992). Historically, research regarding naturally occurring colloids focused on industrial processes. For example, much of water treatment concentrates on the removal of colloidal particles either through flocculation, flotation or filtration. All three processes are fundamentally related to the surface properties of the particles involved (Stumm and Morgan, 1996). In flocculation, coagulants specifically adsorb to the particle surface and alter the surface charge, and coagulant dose is directly related to the total surface area. In flotation, additives render mineral particles hydrophobic, ideally by specific adsorption to surface functional groups with hydrophobic groups exposed to water. Filtration is analogous to coagulation except particles are usually vastly different in size and water is flowing rather than quiescent. The

goal of filtration is to have the colloidal particles attach to larger stationary particles, generally sand grains, within the filtration bed. In this case, removal of the colloidal particles from solution depends on the transport of the particle to the collector (sand grain) and then on the particle-collector interaction (Yao *et al.*, 1971; MacDowell-Boyer, 1992).

More recently, the environmental aspect of colloidal interactions has received attention, particularly as contaminants have been found in groundwater with increasing frequency. Colloids have been implicated as a transport medium for surface and subsurface contaminants (McCarthy and Zachara, 1989). Contaminants thought to be stable and immobile in the soil, such as some agricultural chemicals, radionuclides, and petroleum products, have been observed to move from one area to another (Sheppard *et al.*, 1980; Buddemeier and Hunt, 1988; Mahara and Matsuzuru, 1989; Penrose *et al.*, 1990; Poirrier *et al.*, 1972; Vinten *et al.*, 1983). Colloidal particles to which these contaminants can adsorb are small enough to be mobile, and so the contaminant can also become mobile.

An extensive body of literature exists directly tying the mobility of hydrophobic organic compounds to the presence of stable colloidal material. Many of the early

12

studies described the partitioning of pesticides such as DDT, paraquat, Lindane and others as a function of the amount of organic carbon in the colloidal phase (Poirrier et al., 1972; Gschwend and Wu, 1985; Chiou et al., 1986; Vinten et al., 1983). Although organic matter interacts strongly with pesticides, measurements of organic carbon content can rarely be used alone for predictive purposes because of the intimate association of organic matter with inorganic colloids. In natural environments, most inorganic colloid surfaces are coated with adsorbed natural organic matter which alters the surface charge and aggregation behavior of mineral particles (Kretzschmar and Sticher, 1997; Tipping and Higgins, 1982; Tarchitzky et al., 1993). Such an association may facilitate adsorption of hydrophobic organic contaminants by inorganic constituents. Therefore, it is the combined inorganic-organic colloid interaction that needs to be evaluated in determining the full magnitude of colloid stability and colloid-facilitated contaminant transport.

Although much work has been done on the influence of electrostatic conditions on colloid mobility, particle size and hydrodynamic and filtration effects, less is understood about the role of hydrophobic forces in colloid stability (Elimelech, 1995). This is due, in part, to the difficulty of studying hydrophobic forces in an aqueous system. They can be confused with other forces such as steric interactions, hydration effects or polymer bridging (Israelachvili, 1992). The adsorption of a hydrophobic organic molecule onto the surface of mineral or other inorganic colloids is expected to alter the surface properties and affect the stability of the colloids in aqueous solution. This study evaluated the effects of the grafting of a relatively small hydrophobic organosilane (trimethylchlorosilane) on properties of inorganic colloidal surfaces. The information derived about the treated and untreated surfaces of these colloids helps to elucidate the impact of hydrophobic effects on colloid stability in aqueous solutions.

MATERIALS AND METHODS

Samples

Four minerals and two synthesized inorganic materials were used in this investigation. The minerals included kaolinite (KGa-1, Georgia, well crystallized), montmorillonite (SWy-1, Wyoming), pyrophyllite (Robbins, North Carolina) and MIN-U-SIL® 5 (ground quartz sand, US Silica Company, Berkeley Springs, West Virginia). The kaolinite and montmorillonite are source clays, and a summary of their properties can be found in van Olphen and Fripiat (1979). Pyrophyllite was obtained from Ward's Natural Science (Rochester, New York) in massive form. It was crushed to a powder using an Angstrom ring grinder for a maximum of 5 min.

Particles of appropriate size were isolated by centrifugation (Jackson, 1985). The target particle size was <500 nm for kaolinite, pyrophyllite and MIN-U-SIL® 5 and between 200 and 500 nm for montmorillonite. After centrifugation, the samples were dialyzed to remove excess salts, freeze dried and stored at ambient conditions.

Because pure, naturally occurring, amorphous oxyhydroxide phases of Si and Al are difficult to isolate, synthetic samples are created as reference materials (Goldberg et al., 2001). For synthesis of Al hydroxides, 1 L of 4.0 M NaOH was slowly added to 1 L of 1.5 M AlCl$_3$ while being stirred continuously (Goldberg et al., 2001; Sims and Bingham, 1968). The Si oxide was similarly formed with 2 M Na silicate being stirred continuously as concentrated HCl was added until the solution pH was <7 (Newalkar and Komarneni, 2000). Both the Al hydroxide and Si oxide precipitates were washed to remove excess salts. These samples were used as formed, with no additional treatments.

Silylation

A 5 g sub-sample of each colloid was placed in a Teflon centrifuge tube with 25 mL of 98% pure trimethylchlorosilane (TMCS) obtained from Acros Organics (Fisher Scientific, Pittsburgh, Pennsylvania). The tubes were capped tightly and shaken for 24 h. After shaking, the tubes were uncapped and the samples were allowed to air dry in the hood. Ruiz-Hitzky and Fripiat (1976) suggested that the following grafting reaction occurs between silicate minerals and organochlorosilanes:

$$\equiv Si\text{-}OH \ + \ Cl-\underset{\underset{CH_3}{|}}{\overset{\overset{CH_3}{|}}{Si}}-CH_3 \ \longrightarrow \ \equiv Si\text{-}O-\underset{\underset{CH_3}{|}}{\overset{\overset{CH_3}{|}}{Si}}-CH_3 \ + \ HCl$$

resulting in an organo-mineral derivative. The bond is resistant to hydrolysis and remains stable in aqueous solution. The treated samples were then ground gently and stored in glass containers.

Characterization methods

Once the samples were prepared, various methods were used to determine changes in properties between treated and untreated samples. For simplicity, sample abbreviations are shown in Table 1.

Carbon analysis. The C content of each sample was determined using a Thermo Electron Corporation (Waltham, MA) Flash EA 1112 Series C/N/S analyzer. The detection limit for C is 100 ppm. Sample weights varied between 65 and 95 mg.

Particle size and electrophoretic mobility. Both electrophoretic mobility and particle size were analyzed using a Brookhaven Instruments Corporation ZetaPALS

Table 1. Abbreviations for untreated and treated minerals.

Mineral	Untreated	Treated
Kaolinite	Ka	KaS
Montmorillonite	Mt	MtS
Pyrophyllite	Py	PyS
MIN-U-SIL® 5	Qz	QzS
AlOH-X-ray amorphous	AlOx	AlOxS
SiOx-X-ray amorphous	SiOx	SiOxS

(Holtsville, NY) zeta potential analyzer. Particle size samples were suspended in a 0.001 M NaCl solution at 10 mg of sample to 10 mL of solution and sonicated briefly to enhance dispersion. Five measurements of each sample were made for particle size with an average count rate of 150 kilocounts/s. Electrophoretic mobility was determined with freshly prepared samples at the same suspension concentration (1 mg mL^{-1}) as used in the particle-size determinations in 0.001 M, 0.01 M and 0.1 M NaCl. Each sample was subjected to 10 runs with 10 cycles per run.

Specific surface area. The N$_2$ gas adsorption method was used to determine external (*i.e.* N$_2$ accessible) surface area on each of the samples on a Micromeritics Flowsorb II 2300 (Norcross, GA) surface area analyzer. Each sample was analyzed at least twice, and some sample analyses were duplicated in separate U-tubes. Since the Flowsorb II 2300 reports results as m^2, the SSA was calculated from the measured surface area normalized to the known sample mass.

Cation exchange capacity. A modified Bower method (pH 7.0) was used to determine CEC (Bower and Hatcher, 1966) in which triplicate samples were saturated with a neutral 1 M Na acetate solution and then displaced with a neutral 1 M ammonium acetate solution with a series of three 95% ethanol rinses between. The solutions containing the displaced Na of each sample were then analyzed using an atomic absorption spectrometer (Perkin-Elmer 5000, Wellesley, MA).

Particle aggregation. Each of eight tubes received 250 µL of a suspension of 2.5 g of sample per 100 mL of 0.001 M KCl. An additional 9.5 mL of 0.001 M KCl was added to each tube. The pH was adjusted using either 0.001 M KOH or 0.001 M HCl for a range of pH from 3 to 10. The samples were shaken vigorously to suspend the particles, transferred to spectrophotometer cuvettes and capped. The percent transmittance at 400 nm was then recorded every 30 min for 3 to 4 h on a Spectronic 1000 spectrophotometer (Thermo Electron Corp., Waltham, MA). Care was taken to ensure the samples were not resuspended when adding or removing the cuvettes from the spectrophotometer.

Contact angle (CA). Contact angles were determined with water, di-iodomethane (DIM) and ethylene glycol (EG) on both treated and untreated samples. The powdered samples were adhered to glass slides using the method developed by Bachmann *et al.* (2000).

The CA was measured with an overhead projector tipped on its side to project light onto a paper-covered screen or wall. For the best resolution, the prepared slides were placed perpendicular to, and near the center of, the projector's glass plate surface. The slide projects as a thin line across the screen which was used as the baseline for measurements. A 50 µL drop of liquid was placed on the slide as close to the overhead projector as possible without the drop touching the projector surface. The projector cast an outline of the drop upside down onto the screen which was quickly traced on the paper. Two angles for each drop were determined at the interface of the solid, gas and liquid phases. The angles were then measured with a ruler, pencil and protractor and recorded to the nearest degree.

X-ray diffraction. X-ray diffraction (XRD) patterns were obtained on side-packed, powder-mounted samples using a Siemens (Alpharetta, GA) D500 diffractometer with a CuKα source (α = 0.1542 nm). Each sample was then examined from 2 to 65º2θ with a step size of 0.020º using 1.0 s per step.

Diffuse reflectance infrared Fourier transform (DRIFT) spectroscopy. Samples were combined with KBr to equal 5% sample and 95% KBr, and the resultant mix was ground for 2 min in a mixer mill. The powdered sample was poured into a cylindrical holder and leveled. Spectra were collected using a Mattson Polaris FTIR (Madison, WI) equipped with a mercury cadmium telluride (MCT) detector. Single-beam spectra were obtained by averaging 200 scans at 4 cm^{-1}. The diffuse reflectance accessory, Model DRA-2D was obtained from Harrick Scientific (Ossining, NY) along with a controlled environment chamber, HVC-DRP. The chamber is designed with KBr windows that allow spectra to be taken any time while a continuous flow of gases through the sample is maintained. The chamber was purged with N$_2$ at 1 mL min^{-1}. A mass flow controller was used to maintain flow rates through the sample.

RESULTS AND DISCUSSION

Carbon analysis

Reaction of TMCS with the layer silicates yielded low grafted quantities and low surface coverages (1.2−2.1%) (Table 2). Since the reaction occurs preferentially at silanol sites, the amount of trimethyl silane (TMSi) on the AlOxS surface was below detection. Only on SiOxS did the grafting reaction result in a substantial surface coverage (33%), which made any aqueous analysis of SiOxS difficult. Studies on various silicate

Table 2. Characteristics of untreated and treated colloids.

Colloid	pH 1 mM KCl	iep	TMSi (mmol g^{-1})	TMSi surface coverage (%)	Apparent particle size (nm)	Specific surface area (m^2 g^{-1})	CEC ($cmol_c$ kg^{-1})
Ka	5.2	4.7			451 ± 8^{a}*	18.4 ± 1.1^{a}	18.9 ± 2.7^{a}
KaS	4.7	5.3	0.86	1.4	495 ± 15^{b}	13.7 ± 0.9^{b}	10.7 ± 2.8^{b}
Py	6.2	<3.0			664 ± 10^{a}	46.2 ± 4.6^{a}	27.2 ± 5.0^{a}
PyS	4.9	8.3	3.24	2.1	683 ± 12^{a}	53.5 ± 8.1^{a}	13.5 ± 3.2^{b}
Mt	5.5	<3.0			750 ± 34^{a}	28.6 ± 3.4^{a}	83.4 ± 7.8^{a}
MtS	4.6	<3.0	1.42	1.5	1525 ± 456^{b}	18.0 ± 8.2^{b}	80.3 ± 11.0^{a}
Qz	5.7	3.1			433 ± 3^{a}	19.7 ± 1.5^{a}	3.0 ± 0.1^{a}
QzS	5.4	3.2	5.4	7.5	384 ± 8^{b}	15.3 ± 1.9^{b}	1.6 ± 0.1^{b}
AlOx	4.5	8.4			273 ± 5^{a}	2.5 ± 0.9^{a}	10.5 ± 2.4^{a}
AlOxS	4.3	8.6	<0.01	<0.1	200 ± 3^{b}	11.4 ± 1.5^{b}	2.3 ± 0.2^{b}
SiOx	5.0	<3.0			890 ± 74^{a}	194.2 ± 11.3^{a}	39.6 ± 4.9^{a}
SiOxS	4.4	n.d.[†]	213	33.0	823 ± 34^{a}	124.3 ± 9.0^{b}	3.1 ± 0.5^{b}

* Colloid pairs with different superscripted letters indicate statistical difference at $\alpha = 0.05$ level using a two-tailed t-test.
[†] Not determined

minerals indicate a maximum coverage of 1% C by weight with TMCS silylation (Hair and Hertl, 1969; Ruiz-Hitzky and Fripiat, 1976).

X-ray diffraction

The structure of the minerals (kaolinite, pyrophyllite, montmorillonite and Min-U-Sil®) was unaltered by treatment (data not shown). No major peaks were lost on treatment, peak intensity and shape remained consistent, and only slight peak shifts were observed. Also, grinding did not affect the crystalline integrity of Py. The shift in *d* value between Mt and MtS was so small (<0.01 nm) that we conclude that TMSi did not react with the basal plane (data not shown). With a d_{001} of 1.258 nm and 1.265 nm for Mt and MtS, respectively, each had only a monolayer of water adsorbed in the interlayer space (Chipera and Bish, 2001).

Treatment did impact the structure of X-ray amorphous Al hydroxide, AlOx (data not shown). Untreated AlOx had four identifiable peaks whereas AlOxS had nearly 15 additional new peaks. Treatment appears to have given AlOxS more structure. During silylation, hydrochloric acid is produced which may have solubilized some Al. Upon completion of silylation, the particles may have reformed into a more crystalline structure. Goldberg *et al.* (2001) observed X-ray amorphous Al oxide, which was suspended in water at pH 4 or 5 and shaken for nine days, dissolved and recrystallized as the more stable gibbsite.

SSA and particle size

The grafting of TMSi to Ka, Mt and Qz reduced the SSA and generally increased the particle size (Table 2). The decrease in SSA with treatment is consistent with the increase in particle size although the adsorption of a compound such as TMSi onto the surface will have a minimal effect on size and density as shown with treatment of Py. For SiOx, particle size remained statistically unchanged with treatment though SSA decreased. The SiOxS particles exhibited hydrophobic behavior, thus making suspension in aqueous solution for particle size determination extremely difficult. In this case, the results for SSA, which are performed on powdered samples, are more accurate. Treatment of AlOx produced a decrease in particle size and increase in SSA (Table 2). As discussed previously, exposure of AlOx to TMCS affected the structure of the material which accounts for the reduction in particle size and increase in SSA with treatment.

Cation exchange capacity

Treatment reduced the CECs of all of the samples, though this decrease was not significant for Mt (Table 2). The CEC decreased by >40% for Ka, by ~30% for Py and by >45% for Qz upon treatment. The CEC values for treated and untreated kaolinite were greater than expected. This may be the result of impurities, isolating particles much smaller than the average size for kaolinite, the CEC method selected or a combination of these factors. Even if this is the case, the samples were treated similarly allowing the comparison between treated and untreated samples.

The CEC derives from the adsorption of cations at the surface to satisfy charge developed from either isomorphic substitution during crystal formation or reactive OH functional groups at the surface (Brady and Weil, 2002; Ma and Eggleton, 1999; Sparks, 1995; Sposito, 1984). Isomorphic substitution in layer silicates leads to permanent surface charge which is generally expressed through the siloxane ditrigonal cavity in the tetrahedral sheet (Davis and Kent, 1990; Sposito, 1984). This charge is not pH dependent. Up to 80–90% of the total CEC of

montmorillonite emanates from within the interlayer region between tetrahedral sheets (Ma and Eggleton, 1999; Brady and Weil, 2002; Sposito, 1984). However, these interlayer sites only expose O ions and not the Si-OH groups needed for the grafting reaction (Russell-Colom and Serratosa, 1987). Since TMSi did not react with the interlayer sites, no change in CEC between Mt and MtS is expected.

Variable charge originates from the amphoteric dissociation of surface OH functional groups (Sposito, 1984; Sparks, 1995). The reactivity of surface hydroxyls varies depending upon type and ranges from highly reactive to inactive (Sposito, 1984). Aluminosilicates possess two types of reactive hydroxyls. Aluminol sites ($\equiv$Al-OH) are deprotonated above pH 8 and protonated below pH 8, while silanol sites ($\equiv$Si-OH) are deprotonated at pH above about pH 2 and 3 (Stumm, 1992; Sposito, 1984; Davis and Kent, 1990; Parks, 1962 and Parks, 1990). For a given surface, the point at which the net surface charge is zero, *i.e.* the point of zero charge, is roughly the weighted average of those for aluminols and silanols (Parks, 1990).

During silylation, TMSi reacts with OH functional groups (Wouters *et al.*, 2001). Since more than 95% of the surface charge of Ka and Py and 100% of Qz is determined by reactive hydroxyls (Brady and Weil, 2002; Sposito, 1984), the grafting of TMSi to edge sites blocked access of exchangeable cations and CEC decreased. With CEC determined at pH 7, the aluminol sites were protonated and silanols were deprotonated. Cation exchange occurs at the deprotonated (negatively-charged) sites, so the reduction in CEC implies that TMSi reacted at the silanol edge sites.

The CEC of SiOx and AlOx decreased by 92% and 77%, respectively, following silylation (Table 2). As noted previously, SiOxS was hydrophobic and difficult to suspend in aqueous solution. The CEC of a completely hydrophobic surface would be nil. Recall that the structure of AlOx changed with silylation. Thus, the number and types of exchange sites may have also changed.

Electrophoretic mobility

The electrophoretic mobilities (mobilities) of the untreated samples (except AlOx) were negative for all ionic strengths (0.001 to 0.1 M) and at the pH (~5) (Table 2) conditions evaluated (Figure 1). In contrast, AlOx displayed large positive mobilities at 0.001 and 0.01 M and slightly negative mobility at the highest ionic strength (Figure 1b). Electrophoretic mobilities decreased with increasing ionic strength due to compression of the electric double layer and subsequent reduction in the charge associated with the Stern layer (van Olphen, 1977; Ching *et al.*, 1994; Braggs *et al.*, 1994). As noted previously, it was impossible to measure accurately the mobility of SiOxS as it did not disperse adequately in water.

The mobilities and isoelectric points (ieps) of the organo-mineral colloids were substantially different from the untreated colloids (Figure 1, Table 2). The most dramatic change with treatment was the charge reversal of pyrophyllite. At the lowest ionic strength, untreated pyrophyllite had a mobility of -3.9 μm s^{-1}V^{-1} cm^{-1}, while the mobility for PyS was 4.3 μm s^{-1}V^{-1} cm^{-1} (Figure 1). The iep of pyrophyllite also changed from <pH 3 to pH 8.3 after silylation. This
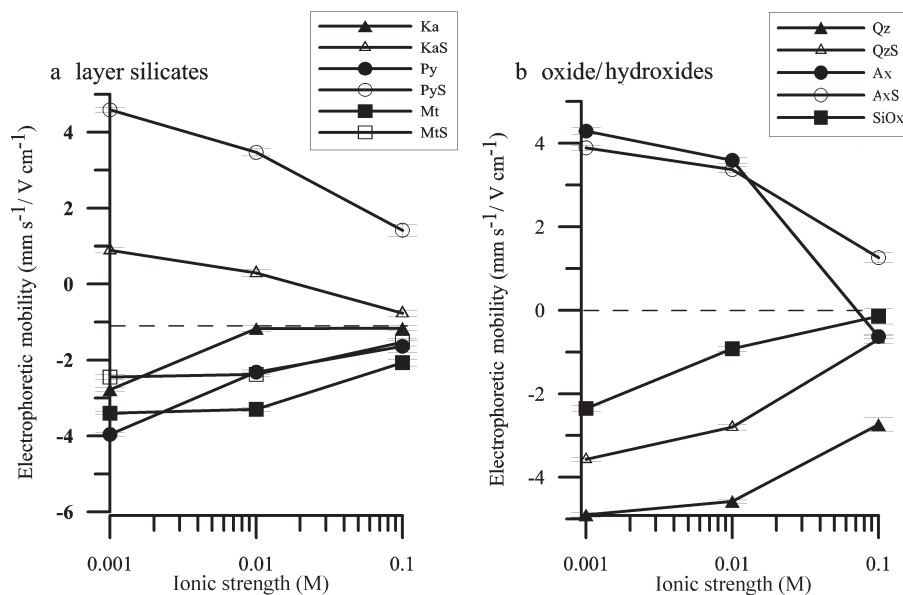

Figure 1. Electrophoretic mobility for treated and untreated (a) layer silicates, and (b) oxide minerals. SiOxS is not shown since its hydrophobicity prevented complete suspension. The pH values at which the suspensions were measured can be found in Table 2.

is additional evidence that TMSi reacted with silanol functional groups. The grafting of TMSi to the particle surface effectively removes the reactive silanol sites (iep = pH 2−3), leaving a greater percentage of aluminol sites (iep = pH 8) available for reactions, thus increasing the positive charge of surface as shown by the increases in ieps (Table 2) (Sposito, 1984, Parks 1962). Since iep is related to the number and type of reactive sites, removal of reactive silanols would cause the overall surface iep to increase, reflecting the greater influence of aluminols on the surface charge (Davis and Kent, 1990). From this, then, fewer silanol sites contributed to the surface charge for KaS, PyS, MS and QzS when TMSi reacted with these sites. While TMCS adsorption to aluminol sites caused the iep to decrease as seen with AlOx and AlOxS, a direct comparison may not be possible due to the change in structure upon silylation which may also affect the number and types of reactive sites.

Contact angle

Contact angles are a convenient means to quantify the relative hydrophobicity or hydrophilicity of a surface. The water contact angles of untreated solids varied from 0° for AlOx (indicating a very highly hydrophilic surface) to 75° for Qz (indicating a weakly wetted surface) (Table 3). Water contact angles for all the treated colloids increased significantly compared to the untreated colloids signifying reduced hydrophilicity (or increased hydrophobicity) due to silylation (Table 3). Contact angles increased more substantially for the oxides (59−114° increase in contact angle) than the layer silicates (18−39°), a result of the greater surface coverage of TMSi (Table 2). The treated silica colloids exhibited the largest angles at 138° for SiOxS and 134° for QzS with PyS having a water contact angle slightly

over 90°. Treatment of Mt had the least effect on water contact angle with a difference of only 18° between Mt and MtS (Table 3).

The results for the untreated phases were well within the range of reported values using more conventional methods. For example, kaolinite (KGa-1b) has a reported water contact angle of 46.1° (Wu, 2001) in reasonable agreement with the value of 34±3° found in this study. Using the sessile drop method and a telemicroscope equipped with an eye piece goniometer, Norris *et al*. (1992) and Costanzo *et al*. (1990) measured contact angles of 38.4° and 42.5°, respectively, for SWy-1 montmorillonite. This also compares favorably with 40° for Mt obtained in this study. Wu (2001) reported a lower value of 33.1° for SWy-2 montmorillonite.

For pyrophyllite, Giese *et al*. (1991) used thin-layer wicking to obtain a contact angle of 79.2°, and using the capillary rise method, Laslett *et al*. (1992) reported an advancing contact angle of 81.4°. These values are larger than that found for Py in this study (55±7°); however, this can be attributed to the method used to examine static contact angles. Bachmann *et al*. (2003) found that the contact angles from the sessile drop method on silt-sized soil samples fell between the advancing and retreating contact angles determined by the Wilhelmy plate method.

Use of alternate liquids provides additional insights into the properties of these surfaces. While in general contact angles using both ethylene glycol (EG) (a polar liquid) and di-iodomethane (DIM) (an apolar liquid) increased with treatment, the value of these measurements is in their use for determining the surface tension and acid-base properties of the samples (Table 3). The mathematical method used is described in detail by Giese *et al*. (1991), Van Oss *et al*. (1988), Costanzo *et al*. (1990) Norris *et al*. (1992) and van Oss and Giese

Table 3. Contact angles of water, ethylene glycol (EG) and di-iodomethane (DIM) with surface tension components for van der Waals (LW), Lewis acid (electron acceptor) (γ^+), Lewis base (electron donor) (γ^-) and Lewis acid/base (AB) properties of the solids.

Mineral	Contact angle (°)			γ^{LW}	γ^+	γ^-	γ^{AB}	ΔG_{iwi}
	Water	EG	DIM		mJ m^{-2}			
Ka	54±3[a]	60±6[a]	40±5[a]	40	1.08	44	14	20
KaS	74±8[b]	58±7[a]	41±3[a]	39	0.02	14	1	−31
Py	55±7[a]	49±4[a]	22±4[a]	47	0.58	33	9	2
PyS	94±7[b]	58±6[b]	37±4[b]	41	0.05	0	0	−103
Mt	40±4[a]	0±0[a]	0±0[a]	51	0.24	36	6	5
MtS	58±13[b]	24±3[b]	27±4[b]	45	0.06	17	2	−26
Qz	75±5[a]	60±3[a]	41±3[a]	39	0.17	14	3	−29
QzS	134±5[b]	121±6[b]	60±4[b]	28	5.64	0	2	−55
AlOx	0±0[a]	42±5[a]	48±5[a]	35	0.22	88	9	76
AlOxS	80±10[b]	60±5[b]	43±4[b]	38	0.04	9	1	−44
SiOx	24±7[a]	28±2[a]	27±3[a]	45	0.08	62	5	46
SiOxS	138±8[b]	127±5[b]	115±6[b]	4	0.06	0	0	−111

* Colloid pairs with different superscript letters indicate statistical difference at α = 0.05 level using a two-tailed t-test.
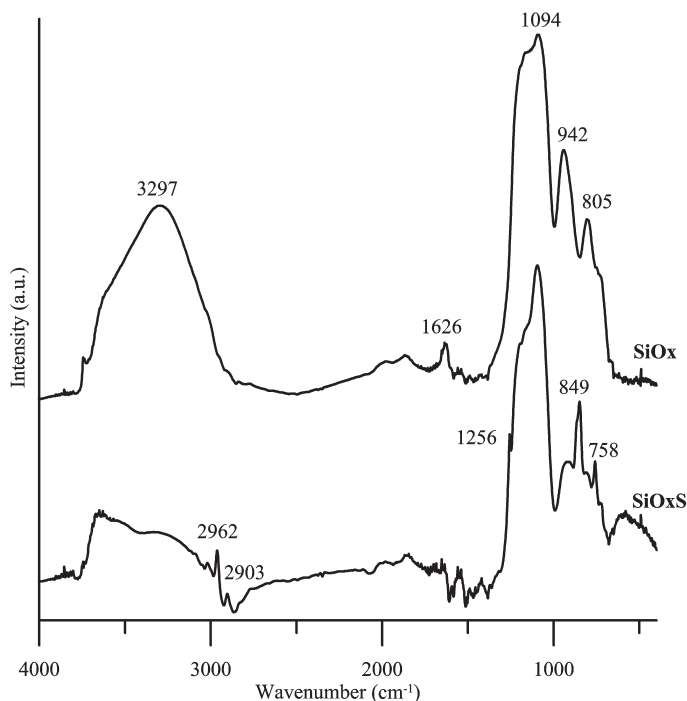
Figure 2. DRIFT spectra comparing treated (SiOxS) and untreated (SiOx) X-ray amorphous silicon oxide.

density, kaolinite readily settles out of suspension at pH values <8 even though the point of zero charge for kaolinite is reported as pH 4.6 (Dixon, 1989; Sparks, 1995; Tama and El-Swaify, 1978). Apparently, TMSi on the kaolinite surface produced limited changes on its aggregation properties since KaS aggregation was similar to that of Ka. Although the iep in this study increased from 4.7 to 5.3 with treatment (Table 2), the change in surface charge was small enough to have minimal effect on KaS stability.

Pyrophyllite and PyS exhibited very different aggregation trends with respect to pH. Pyrophyllite was stable at pH 5 and greater, whereas PyS was stable between pH 3 and 6. At pH 6 and greater, Py was negatively charged (Table 2) creating a stable suspension. As pH decreased below 6, though, Py was less charged and more unstable as it approached its iep near pH 3. Conversely, PyS was positively charged near pH 6 (Table 2) and particles in suspensions at lower pH values had greater positive charge. As pH increased, PyS became less charged. When the net surface charge became sufficiently small (between pH 7 and 9), nothing inhibited particle contact and so particles collided and attached.

When Brownian diffusion controls particle interaction, instability at a specific pH implies the surface charge on the colloid is approaching its point of zero charge (Stumm, 1992; Seta and Karathanasis, 1997; van Olphen, 1977). In other words, rapid aggregation occurs when identical particles carry no net surface charge. At this point, the energy barrier to aggregation is minimal and each collision results in attachment (Elimelech *et*

al., 1995). The point of zero charge is often considered an absolute value, and any deviation increases particle stability. Flocculation, though, can occur in the presence of repulsive electrostatic forces when they are smaller than van der Waals attractive forces (Sposito, 2004). Thus, a range of pH values exists at which the surface charge or surface potential is low enough to cause aggregation (Stumm, 1992). As the surface charge, or the resulting energy barrier, increases, attachment efficiencies decrease and aggregation is slower (Elimelech *et al*., 1995). As a result, the iep changed from <pH = 4 for Py to ~pH = 8 for PyS (Figure 3c,d, Table 2).

Montmorillonite was very stable throughout the experiment, but MtS showed a range of coagulation rates with the division from rapid to slow occurring between pH 6 and 7 (Figure 3e,f). Montmorillonite has permanent negative charge from isomorphic substitution, thus the charge and stability of Mt is independent of solution chemistry, unlike Ka and Py. The covalent bonding of TMSi to the surface reduced the net surface charge (Figure 1), but it had a limited effect on the iep (Table 2). A combination of reduced surface charge and hydrophobic attraction can account for the destabilization of MtS at pH <6. Increasing the pH above 7 increased the negative charge on MtS, stabilizing the suspension.

Min-U-Sil® and SiOx suspensions, like those of Mt, were stable at all pH values. The principle components of both Min-U-Sil® (*i.e.* quartz) and SiOx are O and Si. The iep of both Qz and SiOx were at or below 3. Above
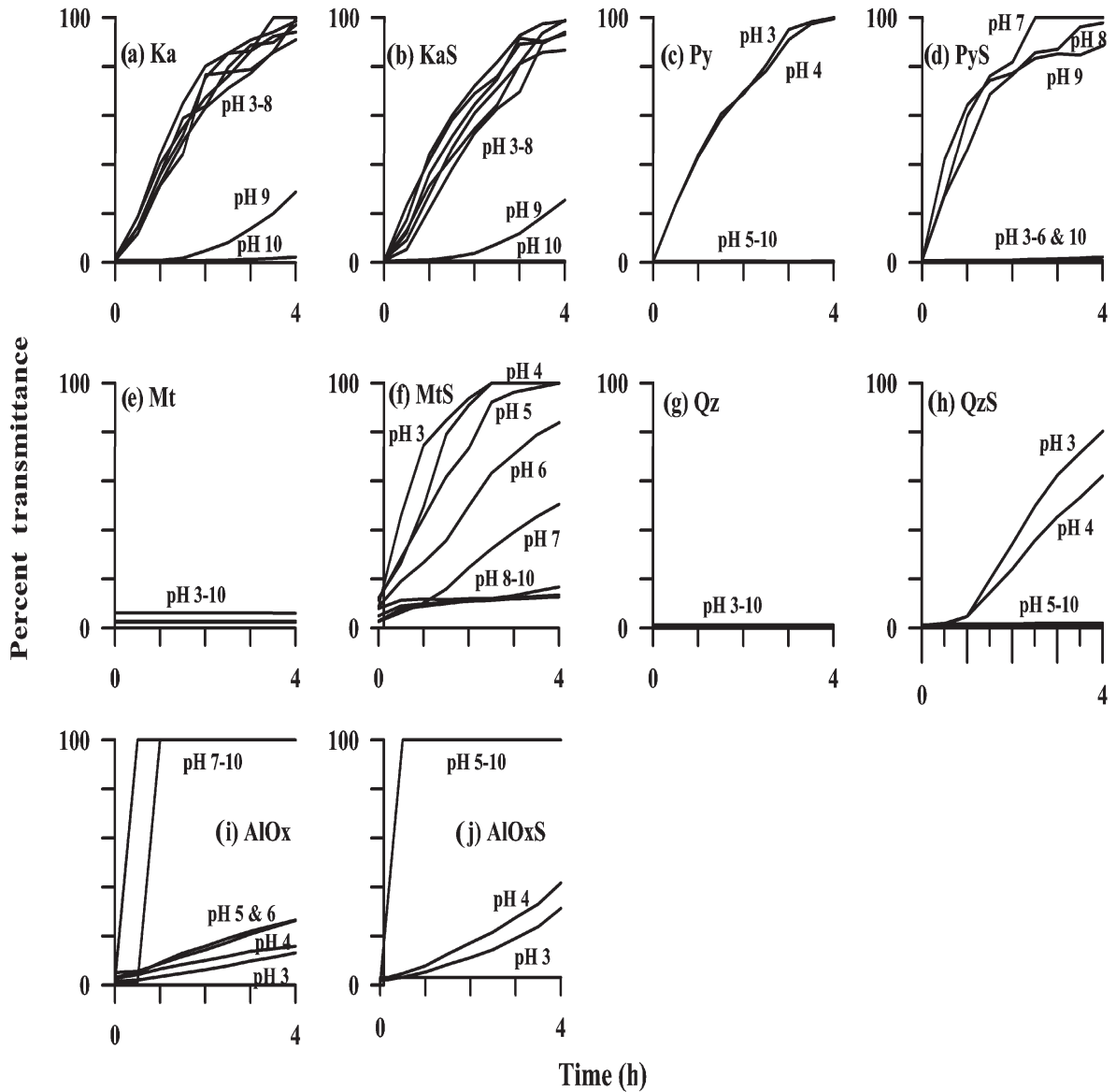
Figure 3. Particle aggregation as a function of pH for (a) kaolinite; (b) silylated kaolinite; (c) pyrophyllite; (d) silylated pyrophyllite; (e) montmorillonite; (f) silylated montmorillonite; (g) Min-U-Sil®; (h) silylated Min-U-Sil®; (i) X-ray amorphous AlOx; and (j) silylated amorphous AlOx. Percent transmittance for SiOx remained near 0 at all pH values and times, yielding a plot similar to Mt (data not shown). SiOxS did not suspend in solution due to its hydrophobic nature.

these pH values, Qz and SiOx particles were negatively charged and repulsive. As a result, the stability of Qz or SiOx was unaffected by pH changes. Rapid coagulation for QzS was observed at pH 3 and 4 (Figure 3h). Similar to MtS, a combination of hydrophobic forces and reduced repulsive forces contributed to QzS aggregation.

For suspensions at pH 7 or greater, AlOx completely aggregated before the second reading (Figure 3i). AlOxS aggregated equally as fast at pH values of 5 or greater (Figure 3j). At pH 4.5 both of these particles were positively charged (Table 2 and Figure 1). As the pH increased, the surface charge decreased until the particles could aggregate. For AlOx, the iep fell between

pH 6 and 7, consistent with gibbsite (Sparks, 1995). Treating the surface with TMCS reduced the charge, albeit only slightly (Figure 1), though it effectively reduced the iep of AlOxS to between pH 4 and 5.

The increase in percent transmittance observed in these experiments is a product of two distinct processes. First, agglomeration involves the transport of particles towards each other, their collision and their attachment. Collision and attachment is a second-order process where the rate constant accounts for the transport of the particles towards each other. The particles then settle out of suspension, which is modeled as a first-order reaction based on Stokes Law of settling. Rate constants

were determined by a best fit to either a first- or second-order reaction from the light scattering plots (data not shown). These rate constants should be considered effective rate constants as they are a combination of agglomeration and settling. For all samples except AlOxS, a first-order reaction was the best fit (data not shown). The dominant process, then, appears to be dominated by settling rather than agglomeration. Effective settling velocities were then compared with theoretical particle velocities based upon Stokes law and primary particle size (Table 4). Assumptions of Stokes law of settling include non-interaction between particles, buoyancy and gravity as the only forces, and settling as a function of particle size and density (Miller and Donahue, 1990).

The settling velocities of Mt and Qz were at least one order of magnitude smaller than the theoretical Stokes velocity which suggests the collision efficiency was small and the particles had sufficient energy to remain suspended against gravity (Table 4). Generally, particles with settling velocities of <0.01 cm s^{-1} remain suspended (Stumm and Morgan, 1996). Settling velocities greater than the theoretical Stokes velocity, such as for Ka or AlOxS, imply that particles collided and attached, with an attachment efficiency near 1. The larger flocculated particles settled faster than anticipated by Stokes law. Rapid coagulation occurred when the settling velocities were >30 times the theoretical Stokes velocity (Figure 3, Table 4). Therefore, a threshold aggregate size is needed for coagulation to occur rapidly.

Particle-settling velocities between the two extremes indicate the complexity of the system. Particles do collide, but the attachment efficiency is <1. As a result, the rate is greater than the theoretical Stokes velocity, but not enough for particles to settle rapidly. Particles with limited changes in concentration exhibited settling velocities within the same order of magnitude as theoretical Stokes velocity. For example, at pH 10 for

Ka, the settling velocity was 0.64 and Stokes velocity was calculated at 0.13 μm s^{-1} (Table 4).

Surface-property modifications

The challenges in predicting colloid properties, especially when exposed to an organic compound, are evident from this study. The adsorption of organic compounds onto a colloidal surface may alter the capacity of the Stern layer, shift the point of zero charge and affect the van der Waals forces (van Olphen, 1977). Therefore, changing the composition of the surface affects the double layer, particle interaction energy and colloid stability. As more than one aspect of the surface changes, the impact of the adsorption of organic compounds on the stability of colloids in aqueous suspension is rather unpredictable. No single property adequately describes the effects of adsorption of organic compounds to the surfaces of environmentally relevant colloids.

In this study, the grafting of TMSi increased the contact angles (θ) for all samples, while the CEC, the polar component of surface tension (γ^{AB}), and the intensity of the IR bands associated with adsorbed water between 3500 and 3200 cm^{-1} (IR$_{3300}$) decreased. The decrease in CEC for Mt, though, was not statistically significant. TMSi covered at most 2% of the surface of the layer silicates, 7.5% of QzS and 33% of SiOxS and was below detection limits for AlOxS. The changes in the apolar component of surface tension (γ^{LW}) were variable. Based on ΔG_{iwi}, all of the treated samples could be considered hydrophobic, though only SiOx was difficult to suspend properly in aqueous solution. As is evident, neither an overall pattern nor one between layer silicates or oxide/hydroxides was discernible. For example, TMSi coverage increased in the order KaS = MtS < PyS, CEC decreased with TMCS treatment in the order of Py > Ka > Mt, but the apolar surface tension (γ^{LW}) decreased as Mt = Py > Ka and contact angle increased Py > Ka > Mt.

Table 4. Calculated settling rate based on particle aggregation. For values <0.01, concentration did not change with time. Values >17 indicate particles settled out of solution within 30 min. Stokes velocity was calculated using $v = \dfrac{d^2 g(\rho_s - \rho_w)}{18\eta}$.

pH	Ka	KaS	Py	PyS	Mt	MtS	Qz	QzS	AlOx	AlOxS	SiOx
					Effective settling velocity (μm s^{-1})						
3	6.78	11.39	11.76	<0.01	<0.01	13.37	<0.01	7.02	1.51	2.87	<0.01
4	7.74	8.62	12.44	<0.01	<0.01	12.16	<0.01	5.18	1.80	2.48	<0.01
5	8.98	6.58	0.06	<0.01	<0.01	3.45	<0.01	<0.01	1.25	>17	<0.01
6	7.64	7.42	<0.01	0.03	<0.01	15.01	<0.01	<0.01	1.87	>17	<0.01
7	10.92	11.47	<0.01	9.33	<0.01	5.54	<0.01	<0.01	>17	>17	<0.01
8	7.08	8.29	<0.01	10.29	<0.01	0.83	<0.01	<0.01	>17	>17	<0.01
9	3.40	3.13	<0.01	4.14	<0.01	0.36	<0.01	<0.01	>17	>17	<0.01
10	0.64	<0.01	<0.01	0.53	<0.01	0.17	<0.01	<0.01	>17	>17	<0.01
Theoretical Stokes velocity	0.13	0.16	0.29	0.30	0.37	0.40	0.12	0.10	0.05	0.03	0.52

In an effort to determine a relationship between changes in surface properties as the result of treatment, a correlation analysis was performed. Interestingly, the change in CEC is as good a predictor of changes in surface properties as the other parameters as the change in CEC (ΔCEC) was correlated (directly or inversely) with all of the other parameters tested at the 90% confidence level (Table 5). In Table 5, 'Δ' is the difference between the treated and the untreated sample of a particular parameter. The covalent bonding of TMSi to the colloidal surface reduced the number of sites available for cation adsorption thus changing the capacity of the Stern layer which impacts W_{adh} and γ^{vw}. As the broken edge sites are generally hydroxylated, the grafting of TMSi to the silanol edge sites eliminated some surface hydroxyls, hence the intensity of IR$_{3300}$ (IR spectra associated with OH groups of adsorbed water) was reduced. Placing methyl groups at sites also affected van der Waals properties, contact angle and the work of adhesion at the surface and so the relationship between these parameters and the change in CEC. The change in contact angle ($\Delta\theta$) is also related to TMSi content, TMSi coverage, the change in the work of adhesion (ΔW_{adh}) and the change in interfacial energy (ΔG_{diff}) with treatment (Table 5). Ironically, ΔG_{diff} was not correlated to TMSi content or TMSi coverage.

Unfortunately, neither the degree of colloid stability nor the conditions of stability can be interpreted solely from changes in surface properties. For example, the contact angle of Ka increased by 19º, CEC decreased by 43% and the iep increased from 4.7 to 5.3 with treatment, yet the aggregate stability study showed little difference between aggregation rates of Ka and KaS. Montmorillonite, on the other hand, had no significant change in CEC or iep and had the smallest change in water contact angle; yet MtS is not a stable colloid in water. The TMSi bonded to the silanol edge sites changed the edge charge from negative to positive. Hence, the attachment of positively charged edges to the negatively charged faces of MtS particles might have been possible.

For pyrophyllite, though, treatment with TMCS caused a dramatic change in iep (from <3 to >8), though CEC decreased by 50% and the contact angle increased by 40º. Silylated Py became unstable when the solution pH was >7 unlike Py which was stable above pH 4. The grafting of TMSi effectively changed the dominant charged species from the silanol to aluminol sites and consequently, PyS aggregation and settling properties resembled those of AlOx. One area not yet considered is the influence of particle shape on surface properties. Several properties of Py suggest that the particle shape may have been less plate-like than either Ka or Mt. Of the three, Py had the greatest reduction in CEC with TMCS treatment and no significant change in particle size or specific surface area. The TMSi content of Py was three times as much as KaS and double that of MtS. This suggests that Py particles have a higher edge-to-face ratio and a more rounded, cylindrical or cubic shape than the more plate-like morphology of Ka and Mt.

Although its contact angle increased by 60º with treatment, the change in stability for QzS occurred only below pH 5 (Figure 3). As it would be stable at the pH of most natural waters, this organo-mineral colloid could be an effective transport medium for both trace elements and organic contaminants.

At pH values >4, AlOxS flocculated rapidly, whereas this only occurred at pHs >6 for the untreated sample. Aluminum is known to be a strong flocculant and is widely used in clarifying processes (Goldberg *et al.*, 1990). Organic compounds like TMCS may actually enhance the flocculation capabilities of Al at lower solution pHs.

CONCLUSIONS

The geochemical fate of most contaminants is controlled by the reaction of the contaminant species with solid surfaces. These adsorption reactions can, in turn, affect the surface properties of suspended particles which further influence their stability and aggregation behavior. TMCS was used as a simple organic probe that

Table 5. Correlation matrix comparing changes with treatment.

	ΔCEC	$\Delta\theta$	ΔW_{adh}	$\Delta\gamma^{LW}$	ΔG_{diff}	ΔIR$_{3300}$	TMSi content	TMSi coverage
ΔCEC	1							
$\Delta\theta$	-0.756^{**}	1						
ΔW_{adh}	0.784^{**}	-0.957^{*}	1					
$\Delta\gamma^{LW}$	0.878^{*}	-0.691	0.827^{*}	1				
ΔG_{diff}	0.763^{**}	-0.776^{**}	0.705	0.514	1			
ΔIR$_{3300}$	0.835^{*}	-0.506	0.532	0.639	0.490	1		
TMSi content	-0.977^{*}	0.773^{**}	-0.847^{*}	-0.959^{*}	-0.683	0.349	1	
TMSi coverage	-0.925^{*}	0.773^{**}	-0.879^{*}	-0.986^{*}	-0.588	-0.726	0.983^{*}	1

* correlated at a 95% confidence level.
** correlated at a 90% confidence level

formed covalent bonds to the broken edge silanol sites of the colloids. By grafting to the edge sites, TMSi affected the surface properties by reducing the CEC of all the solids studied except for Mt. The decrease in CEC with treatment was correlated to the increase in water contact angle, the decrease in interfacial free energy and TMSi content and coverage. The polar components of surface tension decreased for all samples.

The layer silicates had small TMSi coverage which limited interpretation of IR spectra, though decreases in wavenumber positions for OH groups of adsorbed water were observed. With 33% of the SiOxS surface covered with TMSi, the methyl and Si-C bond vibrations were evident in the IR spectra. The isoelectric points increased for all colloids tested. The corresponding reduction in surface reactivity was the direct result of the uncharged methyl groups of TMSi.

Colloidal stability in aqueous environments was reduced except for X-ray amorphous Al hydroxide which became more stable with treatment. The additional hydrophobic nature gained by the samples generally would be sufficient to reduce their transport in the environment. However, at high solution pH, the treated particles would be as easily transported as the untreated minerals. Under such conditions, colloids could facilitate the transport of organic contaminants.

Changes in colloid stability and surface properties of minerals and other inorganic materials after treatment with TMCS implies that the composition, the shape and the size of colloidal materials are important in predicting colloid-facilitated transport of contaminants.

ACKNOWLEDGMENTS

REFERENCES

Bachmann, J., Ellies, A. and Hartge, K.H. (2000) Development and application of a new sessile drop contact angle method to assess soil water repellency. *Journal of Hydrology*, **231−232**, 66−75.

Bachmann, J., Woche, S.K., Goebel, M.-O., Kirkham, M.B. and Horton, R. (2003) Extended methodology for determining wetting properties of porous media. *Water Resources Research*, **39**, 1353−1366.

Buddemeier, R.W. and Hunt, J.R. (1988) Transport of colloidal contaminants in groundwater: radionuclide migration at the Nevada Test Site. *Applied Geochemistry*, **3**, 535−548.

Bower, C.A. and Hatcher, J.T. (1966) Simultaneous determination of surface area and cation exchange capacity. *Soil Science Society of America Proceedings*, **30**, 525−527.

Brady, N.C. and Weil, R.R. (2002) *The Nature and Properties of Soils*, 13th edition. Prentice-Hall, Inc., New Jersey, 960 pp.

Braggs, B., Fornasiero, D., Ralston, J. and St. Smart, R. (1994) The effect of surface modification by an organosilane on the electrochemical properties of kaolinite. *Clays and Clay Minerals*, **42,** 123−136.

Ching, H.W., Tanaka, T.S. and Elimelech, M. (1994) Dynamics of coagulation of kaolin particles with ferric chloride. *Water Resources*, **28**, 559−569.

Chiou, C.T., Malcolm, R.L., Brinton, T.I. and Kile, D.E. (1986) Water solubility enhancement of some organic pollutants and pesticides by dissolved humic and fulvic acids. *Environmental Science and Technology*, **20**, 502−508.

Chipera, S.J. and Bish, D.L. (2001) Baseline studies of The Clay Minerals Society source clays: powder X-ray diffraction analyses. *Clays and Clay Minerals*, **49**, 298−401.

Costanzo, P.M., Giese, R.F. and van Oss, C.J. (1990) Determination of the acid-base characteristics of clay mineral surfaces by contact angle measurements − Implications for the adsorption of organic solutes from aqueous media. *Journal of Adhesion Science Technology*, **4**, 267−275.

Davis, J.A. and Kent, D.B. (1990) Surface complexation modeling in aqueous geochemistry. Pp. 177−260 in: *Mineral-Water Interface Geochemistry* (M.F. Hochella, Jr. and A.F. White, editors). Reviews in Mineralogy Vol. **23**, Mineralogical Society of America, Washington, D.C.

Dixon, J.B. (1989) Kaolin and serpentine group minerals. Pp. 467−535 in: *Minerals in Soil Environments* (J.B. Dixon and S.B. Weed, editors). Soil Science Society of America, Madison, Wisconsin.

Dolphin, D. and Wick, A. (1977) *Tabulation of Infrared Spectral Data*. John Wiley and Sons, New York, 549 pp.

Elimelech, M., Gregory, J., Jia, Z. and Williams, R.A. (1995) *Particle deposition and aggregation: measurement, modeling and simulation.* Butterworth and Heinemann, Oxford, UK, 441 pp.

Gschwend, P.M. and Wu, S. (1985) On the constancy of sediment-water partition coefficients of hydrophobic organic pollutants. *Environmental Science and Technology*, **19**, 90−96.

Giese, R.F., Costanzo, P.M. and van Oss, C.J. (1991) The surface free energies of talc and pyrophyllite. *Physics and Chemistry of Minerals*, **17**, 611−616.

Goldberg, S., Kapoor, B.S. and Rhoades, J.D. (1990) Effect of aluminum and iron oxides and organic matter on flocculation and dispersion of arid zone soils. *Soil Science*, **50**, 588−593.

Goldberg, S., Lebron, I., Suarez, D.L. and Hinedi, Z.R. (2001) Surface characterization of amorphous aluminum oxides. *Soil Science Society of America Journal*, **65**, 78−86.

Hair, M.L. and Hertl, W. (1969) Reaction of chlorosilane with silica surfaces. *Journal of Physical Chemistry*, **73**, 2372−2378.

Israelachvili, J.N. (1992) *Intermolecular and Surface Forces*, 2nd edition. Academic Press, New York, 450 pp.

Jackson, M.L. (1985) *Soil Chemical Analysis−Advanced Course*, 2nd edition, 11th printing. Published by the author, Madison, Wisconsin, 895 pp.

Kretzschmar, R. and Sticher, H. (1997) Transport of humic-coated iron oxide colloids in a sandy soil: Influence of Ca^{2+} and trace metals. *Environmental Science and Technology*, **31**, 3497−3504.

Laslett, R.L., Wansbrough, K.M., Rizzardo, E., Singh, S. and Mainwaring, D.E. (1992) Modification of kaolinite by surface polymerization. *Polymer International*, **28**, 19−23.

Ma, C. and Eggleton, R.A. (1999) Cation exchange capacity of kaolinite. *Clays and Clay Minerals*, **47**, 174−180.

Mahara, Y. and Matsuzuru, H. (1989) Mobile and immobile plutonium in a groundwater environment. *Water Resources*, **23**, 43−50.

Malandrini, H., Clauss, F., Partyka, S. and Douillard, J.M. (1997) Interactions between talc particles and water and organic solvents. *Journal of Colloid and Interface Science*, **194**, 183−193.

McBride, M.B. (1989) Surface chemistry of soil minerals. Pp. 35–159 in: *Minerals in Soil Environments* (J.B. Dixon and S.B. Weed, editors). Soil Science Society of America. Madison, Wisconsin.

McCarthy, J.F. and Zachara, J.M. (1989) Subsurface transport of contaminants. *Environmental Science and Technology*, **23**, 496–502.

McDowell-Boyer, L. (1992) Chemical mobilization of micron-sized particles in saturated porous media under steady flow conditions. *Environmental Science and Technology*, **26**, 586–593.

Miller, R.W. and Donahue, R.L. (1990) *Soils: An Introduction to Soils and Plant Growth*, 6th edition. Prentice-Hall, Inc., New Jersey, 768 pp.

Newalkar, B.L. and Komarneni, S. (2000) Synthesis and characterization of microporous silica prepared with sodium silicate and organosilane compounds. *Journal of Sol-Gel Science and Technology*, **18**, 191–198.

Norris, J., Giese, R.F., van Oss, C.J. and Costanzo, P.M. (1992) Hydrophobic nature of organo-clays as a Lewis acid/base phenomenon. *Clays and Clay Minerals*, **40**, 327–334.

Parks, G.A. (1962) The isoelectric points of solid oxides, solid hydroxides and aqueous hydroxo complex systems. *Chemical Reviews*, **65**, 177–198.

Parks, G.A. (1990) Surface energy and adsorption at mineral/water interfaces: an introduction. Pp. 133–175 in: *Mineral-Water Interface Geochemistry* (M.F. Hochella, Jr. and A.F. White, editors). Reviews in Mineralogy Vol. **23**, Mineralogical Society of America, Washington, D.C.

Penrose, W.R., Polzer, W.L., Essington, E.H., Nelson, D.M. and Orlandini, K.A. (1990) Mobility of plutonium and americium through a shallow aquifer in semiarid region. *Environmental Science and Technology*, **24**, 228–234.

Poirrier, M.A., Bordelon, B.R. and Laseter, J.L. (1972) Adsorption and concentration of dissolved carbon-14 DDT by coloring colloids in surface waters. *Environmental Science and Technology*, **6**, 1033–1035.

Russell-Colom, J.A. and Serratosa, J.M. (1987) Reaction of clays with organic substances. Pp. 371–422 in: *Chemistry of Clays and Clay Minerals* (A.C.D. Newman, editor). Longman Scientific & Technical, Essex, England.

Ruiz-Hitzky, E. and Fripiat, J.J. (1976) Organomineral derivatives obtained by reacting organochlorosilanes with the surface of silicates in organic solvents. *Clays and Clay Minerals*, **24**, 25–30.

Seta, A.K. and Karathanasis, A.D. (1997) Stability and transportability of water-dispersible soil colloids. *Soil Science Society of America Journal*, **61**, 604–611.

Shaw, D.J. (1992) *Colloid and Surface Chemistry*. Butterworth-Heinemann Ltd, Boston, 306 pp.

Sheppard, J.C., Campbell, M.J., Cheng, T. and Kittrick, J.A. (1980) Retention of radionuclides by mobile humic compounds and soil particles. *Environmental Science and Technology*, **14**, 1349–1353.

Sims, J.R. and Bingham, F.T. (1968) Retention of boron by layer silicates, sesquioxides, and soil materials: II. Sesquioxides. *Soil Science Society of America Proceedings*, **32**, 364–369.

Socrates, G. (2001) *Infrared Characteristic Group Frequencies*, 3rd edition. John Wiley and Sons, New York, 347 pp.

Sparks, D.L. (1995) *Environmental Soil Chemistry*. Academic Press, California, 267 pp.

Sposito, G. (1984) *The Surface Chemistry of Soils*. Oxford University Press, New York, 234 pp.

Sposito, G. (2004) *The Surface Chemistry of Natural Particles*. Oxford University Press, New York, 242 pp.

Stumm, W. (1992) *Chemistry of the Solid-Water Interface*. John Wiley & Sons, Inc., New York, 428 pp.

Stumm, W. and Morgan, J.J. (1996) *Aquatic Chemistry: Chemical Equilibria and Rates in Natural Waters*, 3rd edition. John Wiley & Sons, Inc., New York, 1022 pp.

Tama, K. and El-Swaify, S.A. (1978) Charge, colloidal and structural stability interrelationships for oxic soils. Pp. 41–49 in: *Modification of Soils Structure* (W.W. Emerson *et al.*, editors). John Wiley & Sons, New York.

Tarchitzky, J., Chen, Y. and Banin, A. (1993) Humic substances and pH effects on sodium-montmorillonite and calcium-montmorillonite flocculation and dispersion. *Soil Science Society of America Journal*, **57**, 367–372.

Tipping, E. and Higgins, D.C. (1982) The effect of adsorbed humic substances on the colloid stability of hematite particles. *Colloids and Surfaces*, **5**, 85–92.

van Olphen, H. (1977) *An Introduction to Clay Colloid Chemistry for Clay Technologists, Geologists, and Soil Scientists*, 2nd edition. John Wiley & Sons, Inc., New York, 318 pp.

van Olphen, H. and Fripiat, J.J. (1979) *Data Handbook of Clay Materials and other Non-Metallic Minerals*. Pergamon Press, New York, 346 pp.

van Oss, C.J., Chaudhury, M.K. and Good, R.J. (1988) Interfacial Liftshitz-van der Waals and polar interactions in macroscopic systems. *Chemical Reviews*, **88**, 927–941.

van Oss, C.J. and Giese, R.F. (1995) The hydrophobicity and hydrophilicity of clay minerals. *Clays and Clay Minerals*, **43**, 474–477.

Vinten, A.J.A., Yaron, B. and Nye, P.H. (1983) Vertical transport of pesticides into soil when adsorbed on suspended particles. *Journal of Agricultural Food Chemistry*, **31**, 662–664.

Wouters, B.H., Chen, T., Dewilde, M. and Grobet, P.J. (2001) Reactivity of the surface hydroxyl groups of MCM-41 towards silylation with trimethylchlorosilane. *Microporous and Mesoporous Materials*, **44–45**, 453–457.

Wu, W. (2001) Baseline studies of The Clay Minerals Society Source Clays: Colloid and surface phenomena. *Clays and Clay Minerals*, **49**, 446–452.

Yao, K.M., Habibian, M.T. and O'Melia, C.R. (1971) Water and wastewater filtration: concepts and applications. *Environmental Science and Technology*, **5**, 1105–1112.